# The Genetic Requirements for Pentose Fermentation in Budding Yeast

Karin Mittelman[1] and Naama Barkai[1,*]

1 Department of Molecular Genetics, Weizmann Institute of Science, Rehovot 76100, Israel

*Correspondence: naama.barkai@weizmann.ac.il

## Abstract

Cells grow on a wide range of carbon sources by regulating substrate flow through the metabolic network. Incoming sugar, for example, can be fermented or respired, depending on the carbon identity, cell type, or growth conditions. Despite this genetically-encoded flexibility of carbon metabolism, attempts to exogenously manipulate central carbon flux by rational design have proven difficult, suggesting a robust network structure. To examine this robustness, we characterized the ethanol yield of 411 regulatory and metabolic mutants in budding yeast. The mutants showed little variation in ethanol productivity when grown on glucose or galactose, yet diversity was revealed during growth on xylulose, a rare pentose not widely available in nature. While producing ethanol at high yield, cells grown on xylulose produced ethanol at high yields, yet induced expression of respiratory genes, and were dependent on them. Analysis of mutants that affected ethanol productivity suggested that xylulose fermentation results from metabolic overflow, whereby the flux through glycolysis is higher than the maximal flux that can enter respiration. We suggest that this overflow results from a suboptimal regulatory adjustment of the cells to this unfamiliar carbon source.

## Introduction

The budding yeast *Saccharomyces cerevisiae* efficiently adjusts its central metabolism when presented with different nutrients in its environment. In particular, cells can regulate the distribution of carbon flux between fermentation and respiration, depending on carbon quality and availability. Thus, sugars that enter the cell are converted into pyruvate, which can be either directed towards mitochondrial respiration, or be fermented into ethanol (Fig. 1A). The fate of pyruvate at this branch point is determined by the abundance and activity of different metabolic enzymes, which, in turn, are subject to extensive transcriptional and post-transcriptional regulation.

The flexibility of the metabolic network is exemplified by the metabolism of glucose and galactose, two structurally similar hexoses. Glucose is efficiently fermented into ethanol with only little oxygen consumption, while galactose flux is distributed between fermentation and respiration (Velagapudi *et al.* 2007). Indeed, the transcription program activated by each of these sugars is quite different; in particular, glucose triggers a large-scale transcriptional response called glucose repression, characterized by the down-regulation of genes required for respiration or for metabolism of alternative carbon sources. This repression is largely alleviated in galactose-growing cells. In particular, galactose induces several of the glucose-repressed genes for growth (Johnston 1987; Gancedo 2008; Zaman *et al.* 2008).

Budding yeast has been extensively exploited in the bioethanol industry not only because of its efficient fermentation capacity, but also due to its tolerance for high ethanol concentrations and other stresses associated with mass fermentation (Olsson and Hahn-Hägerdal 1993; Olsson and

Nielsen 2000; van Zyl *et al.* 2007). A potential feedstock for bioethanol production is lignocellulose, a polysaccharide found in agricultural crop waste, wood residues and other industrial byproducts. Lignocellulosic biomass consists of approximately 40% hexoses (mostly glucose) and 20% pentoses (mostly xylose). While budding yeast is highly efficient in fermenting the hexose fraction, it does not metabolize xylose, largely reducing the potential ethanol yield from lignocellulose fermentation (Aristidou and Penttilä 2000; Matsushika *et al.* 2009). Attempts to engineer xylose-fermenting *S. cerevisiae* strains face multiple challenges, including the transport of xylose into the cell, isomerization of xylose into the metabolic intermediate xylulose (Hahn-Hägerdal *et al.* 2007; Matsushika *et al.* 2009; Laluce *et al.* 2012), and finally direction of xylulose metabolism towards fermentation, rather than respiration. While many studies have shown that different mutations can improve xylose fermentation by yeast (Kim *et al.* 2013; Sato *et al.* 2016; Bamba *et al.* 2016; dos Santos *et al.* 2016), overcoming the challenge of directing xylulose towards fermentation has received little attention, and requires better understanding of the genes and processes that control central carbon flux.

Despite being rare in the natural environment budding yeast can grow on xylulose as a sole carbon source, enabling a direct study of the means by which cells metabolize this intermediate (MOSES and FERRIER 1962; Gong *et al.* 1981; Chiang *et al.* 1981). Xylulose is transported into the cells via the hexose transporter family, it is then phosphorylated and enters central metabolism through the pentose phosphate pathway (PPP) (Hohenschuh *et al.* 2015). In this study, we systematically screened for metabolic genes that contribute to xylulose fermentation. We find that although xylulose is fermented at considerable yields, cells grown on xylulose activated the transcription program characteristic of respiring cells, and further relied on respiratory genes for growth. Analysis of mutants whose ethanol productivity was diverse revealed that mutants with similar fermentation capacities showed contrasting gene expression programs, and little correlation was found between their fermentation capacity and expression of respiratory genes. Rather, fermentation capacity appeared to correlate with growth rate. The model of overflow metabolism, which suggests that cells direct carbon towards fermentation only after exhausting their respiration capacity, can account for this growth pattern. Based on these results, we suggest that xylulose fermentation is governed by metabolic overflow, likely resulting from a suboptimal regulatory response to this rare carbon source, leading to a limiting respiration capacity.

## Materials and Methods

Yeast Strains and Media

The 411 strains included in our screen were chosen following extensive literature research (Johnston 1987; Olsson and Hahn-Hägerdal 1993; Schüller 2003; Wang *et al.* 2004; Santangelo 2006; Gancedo 2008; Zaman *et al.* 2008, 2009), and include strains deleted for all metabolic enzymes that take part in central carbon metabolism, as well as the regulatory factors that affect these reactions, either directly or indirectly. These genes include sugar transporters, enzymes of glycolysis, gluconeogenesis, the PPP, fermentation, the TCA cycle and the respiratory chain. In addition, genes required for the catabolism of specific carbon sources were screened: galactose, sucrose, fructose, mannose, xylose, arabinose and glycerol. Genes of regulatory networks known to transcriptionally regulate carbon metabolism were included as well: the Ras/PKA network, the Snf1 network, and genes known to specifically regulte the above mentioned pathways, at both the mRNA and protein levels.BY4741 *MATα his3-Δ1 leu2-Δ0 lys2Δ0 met15-Δ0 ura3-Δ0* cells were used as haploid wild type. Strains deleted for the non-essential genes chosen were taken from the Yeast Knockout (YKO) deletion collection (BY4741 genetic background). BY4743 *MATα/α his3Δ1/his3Δ1 leu2Δ0/leu2Δ0 LYS2/lys2Δ0 met15Δ0/MET15 ura3Δ0/ura3Δ0* cells were used as diploid wild type. Heterozygotes for deletions of genes were acquired from the Yeast Magic Marker Collection (BY4743 genetic background).

Deletion strains created for validation experiments were derived from BY4741 using the LiAc/SS DNA/PEG method described by Gietz et al.(Gietz *et al.* 1995). In each strain, the gene deleted was replaced with the kanMX cassette (*geneΔ::KANMX*) using UPTAG and DNTAG primers as described in the Yeast Deletion Project

(http://www-sequence.stanford.edu/group/yeast_deletion_project/usites.html). The deletion was then validated with primers A, B and kanB as described in the project overview.

Strains were grown on standard SC media containing glucose, galactose or xylulose (2%) as a carbon source.

Xylulose Production

A mixture of xylose and xylulose was enzymatically produced from D-xylose as previously described (Gong *et al.* 1981). 350 gr of D-xylose (Sigma X1500) were dissolved in 500 ml DDW and incubated with 20 gr glucose isomerase (Sigma G4166) at 200 rpm for 24 hrs at 60°C. Following incubation the enzyme was inactivated by incubation for 10 min at 100°C. The solution was filtered and relative xylulose concentration was determined by HPLC analysis.

HPLC System

Ethanol production was measured using two Agilent 1200 series HPLC systems, each equipped with a high performance autosampler that enables analysis in 96-well plate format. An anion exchange Aminex HPX-97H column (Bio-Rad, Hercules, CA), which allows measurement of sugar, glycerol and ethanol concentrations, was used to measure sugar concentration in the media. A Fast Acid Analysis column was used for measuring ethanol concentration in the media (allows measuring ethanol concentrations with a retention time of 5 minutes, shorter than 23 minutes when using the Aminex column). . Both columns were eluted with 5mM $H_2SO_4$ at 45ºC. Flow rate for the Aminex column was 0.6 ml/min, flow rate for the Fast Acid Analysis column was 1.0 ml/min.

## Ethanol and Biomass Measurements

Cells were grown in 96-well plates at 30°C in a 96-well plate shaker at 1050 rpm until stationary phase was reached, as determined by preliminary analysis – 24 hours, 40 hours and 13 days on media containing glucose, galactose and xylulose as a carbon source, respectively. Measurements on xylulose were performed after 7 and 10 days of growth as well. Once stationary phase was reached, the cells' OD was measured using a Tecan Sunrise microplate reader, and samples from each well were filtered and frozen at -80°C. Samples were then thawed and placed in the HPLC system for measurement of ethanol concentrations. Ethanol measurements were corrected for ethanol evaporation based on a linear calibration curve.

## Competition Assays

Yeast strains that express a fluorescent marker (e.g. GFP), and a non-fluorescent yeast strain were grown separately overnight. The stationary starters were then inoculated together in the same well of a 96-well plate in equal concentrations, and diluted to a final concentration of 1:1024 of the original starters. The plates were incubated at 30°C in a 96-well plate shaker at 1050 rpm for a time interval that allows the cells to reach stationary phase. Following this time interval, the cells were diluted 1:1024 and again incubated for further growth. This dilution process was repeated in 24 hour intervals for media containing glucose and galactose as a carbon source, and in 72 hour intervals for media containing xylulose. Cell frequency was measured by FACS both at the initial inoculation of the cells in the same well and at each dilution point, measuring 30,000 cells per sample. The differences in the strains' growth rate were derived from the frequencies measured by FACS. The 96-well format allowed high throughput analysis of hundreds of strains in each experiment.

## Flow Cytometry

FACS analysis was done using a BD LSRII system (BD Biosciences). Flow cytometry was conducted with excitation at 488nm and emission at 525±25nm for GFP samples .

## RNA Extraction and Sequencing

A starter of cells was grown overnight on SC medium containing 2% carbon source (glucose, galactose or xylulose). The cells were then diluted to $OD_{600nm}$ = 0.1 in 15 ml tubes and grown until they reached mid log phase ($0.4<OD_{600nm}<0.6$). Cells were then harvested by 1 min centrifugation at 4000 RPM, the supernatant was discarded and they were frozen in liquid nitrogen.

RNA was extracted using the Nucleospin® 96 RNA kit with modifications for working with yeast. Lysis was performed by mixing the cells with 450 µl lysis buffer (1M sorbitol (Sigma S1876), 100 mM EDTA 0.5M, 100 U/ml lyticase). The lysis mixture was transferred to a 96 well plate which was incubated at 30°C for 30 min. The plate was then centrifuged for 10 min at 2500 RPM, and the supernatant was transferred to a 96 well plate provided by the Nucleospin® 96 RNA kit, followed by extraction as described in the kit protocol.

Labeled cDNA was created from RNA extracts, and cDNA was barcoded and then sequenced in the Illumina HiSeq 2500 system, using Truseq SR Cluster Kit v3 -cBot-HS cluster kit and Truseq SBS Kit v3-HS run kit (50 cycles).

## Processing and Analysis of Sequenced RNA

As described in Voichek et al. (Voichek *et al.* 2016).

<u>Data Availability</u>

Table S1 includes a list of all strains included in our screen, as well as all ethanol, OD and competition measurements.  Gene expression data will be available at the SRA database, under BioProject PRJNA381594.

## Results

Screening Metabolic Genes for their Contribution to Xylulose Growth and Fermentation

We chose 411 metabolic enzymes and regulatory factors associated with central carbon metabolism (Fig. 1A), and screened for those that affect growth or fermentation on glucose, galactose and xylulose (Table S1). This was done by assembling a collection of strains that are deleted or heterozygote for the non-essential or essential genes, respectively.

Temporal analysis of ethanol production and sugar depletion revealed that wild-type cells grown on 2% glucose consumed the sugar within 24 hours, producing 7 gr/l of ethanol (Figs. 1B, S1), which corresponds to ~70% of the theoretical yield (Zhang *et al.* 2015). Growth on galactose produced a similar amount of ethanol but at a slower rate, depleting the sugar only after ~40 hours of growth. Growth on 2% xylulose was significantly slower: after 13 days of growth, xylulose could still be detected in the medium. Still, a significant amount of ethanol was produced (4.5 gr/l), corresponding to ~65% of the ethanol yield on glucose.

The mutant strains were similarly characterized, by measuring the OD and the amount of ethanol produced from the three carbon sources.. On xylulose, two additional time points were taken to assess ethanol production and OD during mid-logarithmic growth as well. We further measured the growth rates of all mutant strains in the three conditions studied using a sensitive competition assay (Fig. 1C, Table S1). Mutant strains were co-incubated with GFP-labeled wild-type cells, and their relative abundance was quantified by flow cytometry at stationary phase. The relative growth rate was calculated by measuring these frequencies temporally, following several dilutions of the cultures. Growth on Xylulose Shows a Signature of Respiratory Metabolism

Of the 411 strains examined, 55 were non-viable (or showed very poor growth) on xylulose. Of these, 30 were non-viable also on galactose. Of the 25 remaining mutants, previous analysis indicated that 21 were non-viable on glycerol, a carbon source that can only be respired but not fermented (McAlister-Henn and Thompson 1987; Dimmer *et al.* 2002; Dudley *et al.* 2005; Merz and Westermann 2009; Na *et al.* 2014) (Table S2). Therefore, only four genes were essential specifically for growth on xylulose: *TKL1*, *TAL1*, *PFK2* and *TDH1* (Fig. 2B).

The majority of the 30 genes that were essential for growth on both galactose and xylulose (but not on glucose) are involved in the electron transport chain or participate in its regulation (Fig. 2A, left panel). Similarly, the majority of the 25 strains that were non-viable on both xylulose and glycerol were again associated with the respiratory pathways, including the TCA cycle and the electron transport chain. In addition, several of these genes were part of the Snf1 regulatory network, which is responsible for deactivating the glucose repression response (Schüller 2003). Therefore, despite the considerable ethanol yield during growth on xylulose, growth on this sugar depended on respiratory genes in a manner highly similar to that of growth on carbon sources that are strictly respired, such as glycerol.

To better understand this requirement for respiratory genes, we asked whether a respiratory signature is evident also in the pattern of gene expression. To this end, we measured the genome-wide transcription programs of wild-type cells growing on xylulose and glucose. Consistent with the genetic requirements described above, genes of the TCA cycle, electron transport chain, and gluconeogenesis were highly induced on xylulose compared to glucose (Figs. 2B-C). Further, the expression pattern on xylulose was most similar to that of cells grown on the strictly respiratory carbon ethanol, as evident by comparison of this expression program

to that reported on multiple carbon sources (Fig. 2D, (Gasch *et al.* 2000)). In addition to ethanol, these carbon sources also included the fermentative sugars glucose, sucrose and mannose, and the partially respiratory sugars galactose and raffinose. Taken together, both the genetic requirements and the gene expression signature were indicative of a largely respiratory metabolism of xylulose, despite high ethanol yield.

Enzymes that Link Glycolysis to the Pentose Phosphate Pathway are Essential for Growth on Xylulose

As described above, of the 55 genes that were essential for growth on xylulose, four were not essential for growth on either glycerol or galactose: *TKL1*, *TAL1*, *PFK2* and *TDH1*. As we describe below, these genes are positioned at critical nodes, linking the PPP with glycolysis through intermediates common to both pathways, and may therefore be required to allow the entry of carbon to central metabolism through the PPP.

Two of these genes, *TAL1* and *TKL1*, catalyze PPP reactions required for conversion of xylulose into glycolytic intermediates (Fig. 2A, right panel): Tkl1 converts xylulose-5-phosphate and ribose-5-phosphate into sedoheptulose-7-phosphate and glyceraldehyde-3-phosphate (GA-3-P), while Tal1 converts the latter two into erythrose-4-phosphate and fructose-6-phosphate (Fru-6-P) (Fig. S2). In addition to their role in the PPP, there is evidence indicating that over-expression of these two genes can drive ethanol production in several different growth conditions (Hasunuma *et al.* 2014; Cao *et al.* 2014; Kobayashi *et al.* 2017), although *TAL1* expression was not significantly induced during growth on xylulose compared to glucose (Fig. 2C). *TKL1* was slightly down-regulated, while its paralog, *TKL2*, was induced (Fig. 2C). This induction of the minor transketolase isoform was therefore not able to compensate for the *TKL1* deletion, in agreement with early studies of the two enzymes in which the Δ*tkl1* mutant showed immeasurable transketolase activity (SCHAAFF-GERSTENSCHLAGER *et al.* 1993). In addition, Tkl1 is primarily localized to the nucleus, while Tkl2 is primarily localized to the cytoplasm (Koh *et al.* 2015), suggesting a functional difference between the two, perhaps a role in nucleotide production, for which the PPP is responsible.

The two additional genes that were required specifically for growth on xylulose code for enzymes of the glycolysis pathway: *PFK2* and *TDH1* (Fig. 2A, right panel). *TDH1* encodes one of three glyceraldehyde-3-phosphate dehydrogenase isozymes, which catalyze the conversion of GA-3-P to 1,3-bis-phosphoglycerate in glycolysis. *PFK2* encodes the beta subunit of phosphofructokinase, another key enzyme of glycolysis that catalyzes the formation of fructose 1,6-bisphosphate from Fru-6-P. These two enzymes link the PPP with glycolysis, allowing xylulose to enter central carbon metabolism, likely justifying their essentiality for growth on xylulose (Fig. 2A, right panel).

During growth on glucose or galactose, Δ*pfk2* and Δ*tdh1* grew at the same rate as wild-type cells, suggesting that their depletion is efficiently compensated for by their respective isozymes. The strict requirement for *TDH1* on xylulose may be explained by its expression pattern: while *TDH1* was induced on xylulose compared to glucose, its two isozymes, *TDH2* and *TDH3*, were not (Fig. 2C). This expression pattern was consistent with that observed under stress or respiratory conditions (Gasch *et al.* 2000; Delgado *et al.* 2001).

In contrast, the expression of *PFK2*, or of its isozyme *PFK1*, was not noticeably different between by xylulose and glucose (Fig. 2C). However, *FBP1*, which catalyzes the reverse reaction in

gluconeogenesis, was induced on xylulose, perhaps explaining why both enzymes were needed to maintain the directionality of the glycolytic flux downstream, towards energy and biomass production. Notably, this induction pattern has also been observed under stress or respiratory conditions (Gasch *et al.* 2000; Delgado *et al.* 2001).

Exploring Genes that Alter Xylulose Fermentation:

We next searched for mutants that maintained growth on xylulose, but were perturbed in their fermentation capacity, producing less (or more) ethanol than wild-type cells. Our screen pointed to 39 candidates, for which we generated the mutations anew, and measured their ethanol production, biomass and growth rate on xylulose. Twenty of these strains, which showed the most consistent results, were kept for further analysis (Figs. 3A, S3A, Table S3).

We classified the mutants into three groups (Figs. S4-6, Tables S3, S4). First, we included six strains that produced low amounts of ethanol and reached a low final OD, giving specific ethanol productivity that was lower than wild type. This phenotype indicated a general deficiency of growth on xylulose. Genes assigned to this group were *XKS1, PFK1, ISF1, SHR5, PRS3 andTPK1.* Xks1 is the xylulokinase enzyme that converts D-xylulose and ATP to xylulose-5-phosphate and ADP (Richard *et al.* 2000), and it was therefore expected that the ethanol productivity of its heterozygote deletion was low (Fig. 3B). Low ethanol yield was also found for the strain deleted of *PFK1*, the α subunit of phosphofructokinase, whose β subunit was found to be essential for growth on xylulose. Second, we considered strains that produced less ethanol than wild type cells, while reaching the same final OD. Genes assigned to this group were *TPK3, ALD4, ACH1,* and *COX5A.* These mutants appeared to divert flux away from fermentation (Fig. 3C). The final group of strains produced wild type-like amounts of ethanol but reached a lower final OD, indicating increased specific ethanol productivity (Fig 3D). Genes assigned to this group included *IRA2, NRG1, SAK1, EXG1, IDH2, PDA1, LSC2, GID8, LSC1* and *ADH3*. Notably, none of the selected strains were deficient in growth on glucose or galactose (Fig. S3B). Expression of fourteen of these twenty genes was up regulated by xylulose, as compared to glucose (Fig. S7).

Growth on Xylulose Induces Respiratory and Stress Related Genes in Mutant Strains

As can be seen, the selected mutants were associated with different metabolic functions (Fig. 3A, Table S3). Since fermentation yield correlates with a well-defined transcription program, we asked whether the mutants show a consistent expression signature that correlates with their effects. To this end, we compared the gene expression program of each mutant when grown on glucose and xylulose. All mutants responded to the transfer to xylulose-containing media in essentially the same way: they induced respiratory genes such as those of the TCA cycle and electron transport chain, up-regulated specific isozymes of the PPP, and down-regulated ribosomal-associated genes (Fig. 3E). Therefore, the mutant phenotypes were not explained by differential regulation of gene expression between glucose and xylulose.

We next asked whether mutant fermentative capacity correlated with absolute expression levels of respiratory genes on glucose or on xylulose. No correlation was identified when comparing the ethanol yield of the different strains and the associated expression levels of genes in the TCA cycle, electron transport chain or PPP (Fig. 4A). This lack of correlation was consistent with previous results from our lab, comparing xylulose fermentation in different wild-type strains (Tamari *et al.* 2014), as well as with other studies that have shown induction of

genes associated with metabolism of non-fermentable carbon sources (Scalcinati *et al.* 2012; Shen *et al.* 2013; Alff-Tuomala *et al.* 2016; Sato *et al.* 2016). Similarly, no correlation was identified between growth rate of the mutants and the expression of growth-associated genes: genes induced or down regulated by the environmental stress response (ESR-induced and ESR-reduced, respectively), stress genes, and ribosomal biogenesis genes (Ribi)(Fig. 4B). Also consistent with previous results, growth rates were positively correlated with the expression of ribosomal proteins (RP) (c=0.69), and negatively correlated with expression of amino-acid biosynthesis genes (AA)(c=-0.57).This negative correlation with AA genes was previously described in cells growing on xylulose, as well as deletion mutants and yeast growing on several drugs (Tamari *et al.* 2014). Common to all of these conditions and genetic perturbations is a lack of evolutionary adaptation, which may lead to differential expression patterns of growth associated genes.

Together, we show that expression patterns of mutants perturbed in their fermentation capacity did not correlate with ethanol production, and that their growth rates were not correlated with growth associated genes. In addition, respiratory and stress genes were induced, again indicating that ethanol production occured despite a respiratory gene expression program.


Strains with Similar Phenotypes Show Contrasting Expression Patterns

The lack of correlation between specific ethanol productivity and the expression of respiratory genes was surprising to us, and we therefore examined more directly whether mutants assigned to the same phenotypic class also showed consistent expression patterns (Fig. S8). To this end, we systematically screened for differential expression of gene modules, defined by co-expression or co-functionality (Ihmels *et al.* 2002). However, we could not detect consistent expression changes that distinguished the different phenotypic classes.

As a specific example, consider the mutants $\Delta ira2$ and $\Delta idh2,$ both of which showed increased specific ethanol productivity compared to wild type cells (Fig. 4C). Despite showing a similar phenotype, their expression pattern was largely different (Fig. 4D): $\Delta ira2$ down regulated stress genes and induced the RP and Ribi genes. By contrast, $\Delta idh2$ up regulated stress genes and down regulated RP and Ribi genes. This opposite expression pattern is consistent with gene function: Ira2 is a GTPase-activating protein that is a negative regulator of the Ras pathway. Deletion of *IRA2* therefore results in a constitutively active Ras (Wang *et al.* 2004; Zaman *et al.* 2008) which mimics high-glucose conditions, and has also been shown to improve xylose fermentation (Sato *et al.* 2016). Idh2, one the other hand, is a subunit of the mitochondrial isocitrate dehydrogenase complex that catalyzes the oxidation of isocitrate to α–ketoglutarate in the TCA cycle. Disruption of this complex likely impairs the flux through the TCA cycle, necessitating further induction of respiratory and stress genes.

Our data also included strains whose phenotype was distinct, but showed similar gene expression patterns. An example is $\Delta ira2$, described above, and $\Delta pfk1$, which showed decreased specific ethanol productivity compared to the wild type (Fig. 4C,D). Therefore, no correlation could be detected between the gene expression pattern and the ethanol production phenotype in this case either.


Xylulose Fermentation: A Signature of Overflow Metabolism

Gene expression patterns therefore showed little correlation with the mutants' fermentation or growth capacity. This may suggest a more global control of fermentation capacity, perhaps in association with the strains' growth rate. To examine this, we asked whether the specific ethanol productivity correlated with the strains' growth rate, as measured in a sensitive competition assay. During growth on xylulose the specific ethanol productivity of the different strains, as measured after 7 days of growth, was well correlated with their growth rate (Fig. 4E, c=0.51). Notably, this correlation was specific to growth on xylulose, but was not observed during growth on glucose or galactose.

Correlation between growth rate and ethanol yield has previously been reported for cells growing in continuous cultures limited for glucose (Kaspar von Meyenburg 1969; Postma *et al.* 1989). As a possible explanation, the model of metabolic overflow was proposed. Within this model, respiration occurs at a maximum rate, with any additional flow exceeding this capacity being directed towards fermentation (Vemuri *et al.* 2007). When interpreted in this context, our data suggests that xylulose influx changes in proportion to cell growth rate, while the flux directed towards respiration remains constant, at its maximal limit. Mutants that reduced growth rate therefore directed a larger proportion of their incoming flux towards respiration, leading to reduced specific ethanol productivity.

## Discussion

In this study, we characterized the growth of budding yeast on xylulose, the only known pentose which these cells can naturally utilize. Xylulose is not widely available in nature, yet its incorporation into the metabolic network is possible as it is a natural intermediate of the PPP. Through the PPP, xylulose is fed into the lower part of glycolysis and from there it can be directed towards fermentation or respiration. Notably, under the conditions of our study, a significant fraction of the xylulose carbon was indeed directed into fermentation, reaching a high yield corresponding to 65% of the ethanol yield on glucose.

Despite this significant ethanol production, growth on xylulose was dependent on genes essential for growth on non-fermentable carbon sources (but not required during growth on glucose or on galactose). Therefore, respiration plays a critical role in xylulose metabolism. This reliance on respiratory genes is reflected in, and perhaps explained by, the gene expression pattern, which again mostly resembled that of cells growing on a purely respiratory carbon source, such as ethanol. Therefore, it appears that cellular regulatory networks controlling gene expression and function are not properly tuned for metabolizing xylulose, consistent with its rarity in nature.

We noted that in most of our deletion strains, the specific ethanol productivity was proportional to the strain's growth rate (Fig. 4E). We interpreted this observation in the context of the model of metabolic overflow (Vemuri *et al.* 2007), which assumes that flow through respiration is limited, so that any excess of incoming flux beyond this limit is directed towards fermentation. In this context, our findings suggested that in most mutants the flux through glycolysis, upstream of the pyruvate branch point, changed in proportion to cell growth rate, while the respiration threshold remained invariant. Therefore, when a mutant decreased growth rate, it also decreased the flux going through glycolysis, thereby lowering the overflow flux used for ethanol production.

As an exception to this general rule, we noted a group of genes that increased ethanol production but did not increase growth rate (Fig. 4E). Within the overflow models, these mutants were expected to affect not only the flux through upper glycolysis, but also the threshold-flux entering respiration. Indeed, $\Delta ira2$, for example, reduced expression of respiratory genes, thereby limiting the carbon flux that is directed towards respiration. By contrast, deletion of genes of the respiratory pathway, downstream of the pyruvate branch point, such as $\Delta idh2$, may have limited the respiratory flux more directly, by limiting the function of the associated pathway.

Remarkably, none of our deletion mutants produced more ethanol than the wild type. Strains that produced wild type levels of ethanol at a lower final OD had increased specific ethanol productivity by definition, yet the overall yield did not increase. Further, the overall correlation we observed between the amount of ethanol produced and cell growth rate was specific to growth on xylulose, but was not observed during growth on glucose or galactose. In fact, during growth on these two carbon sources, the strains showed little variability in their ethanol production and the final OD that they reached (Fig. 1C).

Studying the growth of mutant strains when provided with xylulose as a sole carbon source has given us novel insight into the processes that occur in the cell when carbon enters central metabolism through the PPP. Our results indicate that this special carbon source can be fermented and yet induces and requires respiratory and gluconeogenic genes. This raises the possibility that decoupling the regulation of respiration and gluconeogenesis may better tune

pentose metabolism towards fermentation. The cell, however, appears highly robust against such perturbations, suggesting that this coupling provided a significant benefit during yeast evolution.

## References

Alff-Tuomala, S., L. Salusjärvi, D. Barth, M. Oja, M. Penttilä *et al.*, 2016 Xylose-induced dynamic effects on metabolism and gene expression in engineered Saccharomyces cerevisiae in anaerobic glucose-xylose cultures. Appl. Microbiol. Biotechnol. 100: 969–985.

Aristidou, A., and M. Penttilä, 2000 Metabolic engineering applications to renewable resource utilization. Curr. Opin. Biotechnol. 11: 187–98.

Bamba, T., T. Hasunuma, and A. Kondo, 2016 Disruption of PHO13 improves ethanol production via the xylose isomerase pathway. AMB Express 6: 4.

Cao, L., X. Tang, X. Zhang, J. Zhang, X. Tian *et al.*, 2014 Two-stage transcriptional reprogramming in Saccharomyces cerevisiae for optimizing ethanol production from xylose. Metab. Eng. 24: 150–159.

Chiang, L. C., H. Y. Hsiao, P. P. Ueng, and G. T. Tsao, 1981 Enzymatic and Microbial Preparation of d-Xylulose from d-Xylose. Appl. Environ. Microbiol. 42: 66–9.

Delgado, M. L., J. E. O'Connor, I. Azorín, J. Renau-Piqueras, M. L. Gil *et al.*, 2001 The glyceraldehyde-3-phosphate dehydrogenase polypeptides encoded by the Saccharomyces cerevisiae TDH1, TDH2 and TDH3 genes are also cell wall proteins. Microbiology 147: 411–7.

Dimmer, K. S., S. Fritz, F. Fuchs, M. Messerschmitt, N. Weinbach *et al.*, 2002 Genetic basis of mitochondrial function and morphology in Saccharomyces cerevisiae. Mol. Biol. Cell 13: 847–53.

Dudley, A. M., D. M. Janse, A. Tanay, R. Shamir, and G. M. Church, 2005 A global view of pleiotropy and phenotypically derived gene function in yeast. Mol. Syst. Biol. 1: 2005.0001.

Gancedo, J. M., 2008 The early steps of glucose signalling in yeast. FEMS Microbiol. Rev. 32: 673–704.

Gasch, A. P., P. T. Spellman, C. M. Kao, O. Carmel-Harel, M. B. Eisen *et al.*, 2000 Genomic expression programs in the response of yeast cells to environmental changes. Mol. Biol. Cell 11: 4241–57.

Gietz, R. D., R. H. Schiestl, A. R. Willems, and R. A. Woods, 1995 Studies on the transformation of intact yeast cells by the LiAc/SS-DNA/PEG procedure. Yeast 11: 355–360.

Gong, C. S., L. F. Chen, M. C. Flickinger, L. C. Chiang, and G. T. Tsao, 1981 Production of Ethanol from d-Xylose by Using d-Xylose Isomerase and Yeasts. Appl. Environ. Microbiol. 41: 430–6.

Hahn-Hägerdal, B., K. Karhumaa, C. Fonseca, I. Spencer-Martins, and M. F. Gorwa-Grauslund, 2007 Towards industrial pentose-fermenting yeast strains. Appl. Microbiol. Biotechnol. 74: 937–953.

Hasunuma, T., K. S. K. Ismail, Y. Nambu, and A. Kondo, 2014 Co-expression of TAL1 and ADH1 in recombinant xylose-fermenting Saccharomyces cerevisiae improves ethanol production from lignocellulosic hydrolysates in the presence of furfural. J. Biosci. Bioeng. 117: 165–169.

Hohenschuh, W., R. Hector, and G. S. Murthy, 2015 A dynamic flux balance model and bottleneck identification of glucose, xylose, xylulose co-fermentation in Saccharomyces cerevisiae. Bioresour. Technol. 188: 153–160.

Ihmels, J., G. Friedlander, S. Bergmann, O. Sarig, Y. Ziv *et al.*, 2002 Revealing modular organization in the yeast transcriptional network. Nat. Genet. 31: 370–7.

Johnston, M., 1987 A model fungal gene regulatory mechanism: the GAL genes of Saccharomyces cerevisiae. Microbiol. Rev. 51: 458–76.

Kaspar von Meyenburg, H., 1969 Energetics of the budding cycle of Saccharomyces cerevisiae during glucose limited aerobic growth. Arch. Mikrobiol. 66: 289–303.

Kim, S. R., J. M. Skerker, W. Kang, A. Lesmana, N. Wei *et al.*, 2013 Rational and Evolutionary Engineering Approaches Uncover a Small Set of Genetic Changes Efficient for Rapid Xylose Fermentation in Saccharomyces cerevisiae (S. S. Fong, Ed.). PLoS One 8: e57048.

Kobayashi, Y., T. Sahara, T. Suzuki, S. Kamachi, A. Matsushika *et al.*, 2017 Genetic improvement of xylose metabolism by enhancing the expression of pentose phosphate pathway genes in Saccharomyces cerevisiae IR-2 for high-temperature ethanol production. J. Ind. Microbiol. Biotechnol.

Koh, J. L. Y., Y. T. Chong, H. Friesen, A. Moses, C. Boone *et al.*, 2015 CYCLoPs: A Comprehensive Database Constructed from Automated Analysis of Protein Abundance and Subcellular Localization Patterns in Saccharomyces cerevisiae. G3 (Bethesda). 5: 1223–32.

Laluce, C., A. C. G. Schenberg, J. C. M. Gallardo, L. F. C. Coradello, and S. R. Pombeiro-Sponchiado, 2012 Advances and Developments in Strategies to Improve Strains of Saccharomyces cerevisiae and Processes to Obtain the Lignocellulosic Ethanol–A Review. Appl. Biochem. Biotechnol. 166: 1908–1926.

Matsushika, A., H. Inoue, T. Kodaki, and S. Sawayama, 2009 Ethanol production from xylose in engineered Saccharomyces cerevisiae strains: current state and perspectives. Appl. Microbiol. Biotechnol. 84: 37–53.

McAlister-Henn, L., and L. M. Thompson, 1987 Isolation and expression of the gene encoding yeast mitochondrial malate dehydrogenase. J. Bacteriol. 169: 5157–66.

Merz, S., and B. Westermann, 2009 Genome-wide deletion mutant analysis reveals genes required for respiratory growth, mitochondrial genome maintenance and mitochondrial protein synthesis in Saccharomyces cerevisiae. Genome Biol. 10: R95.

MOSES, V., and R. J. FERRIER, 1962 The biochemical preparation of D-xylulose and L-ribulose. Details of the action of Acetobacter suboxydans on D-arabitol, ribitol and other polyhydroxy compounds. Biochem. J. 83: 8–14.

Na, U., W. Yu, J. Cox, D. K. Bricker, K. Brockmann *et al.*, 2014 The LYR factors SDHAF1 and SDHAF3 mediate maturation of the iron-sulfur subunit of succinate dehydrogenase. Cell Metab. 20: 253–66.

Olsson, L., and B. Hahn-Hägerdal, 1993 Fermentative performance of bacteria and yeasts in lignocellulose hydrolysates. Process Biochem. 28: 249–257.

Olsson, and Nielsen, 2000 The role of metabolic engineering in the improvement of Saccharomyces cerevisiae: utilization of industrial media. Enzyme Microb. Technol. 26: 785–792.

Postma, E., C. Verduyn, W. A. Scheffers, and J. P. Van Dijken, 1989 Enzymic analysis of the crabtree effect in glucose-limited chemostat cultures of Saccharomyces cerevisiae. Appl. Environ. Microbiol. 55: 468–77.

Richard, P., M. H. Toivari, and M. Penttilä, 2000 The role of xylulokinase in Saccharomyces cerevisiae xylulose catabolism. FEMS Microbiol. Lett. 190: 39–43.

Santangelo, G. M., 2006 Glucose Signaling in Saccharomyces cerevisiae. Microbiol. Mol. Biol. Rev. 70: 253–282.

dos Santos, L. V., M. F. Carazzolle, S. T. Nagamatsu, N. M. V. Sampaio, L. D. Almeida *et al.*, 2016 Unraveling the genetic basis of xylose consumption in engineered Saccharomyces cerevisiae strains. Sci. Rep. 6: 38676.

Sato, T. K., M. Tremaine, L. S. Parreiras, A. S. Hebert, K. S. Myers *et al.*, 2016 Directed Evolution Reveals Unexpected Epistatic Interactions That Alter Metabolic Regulation and Enable Anaerobic Xylose Use by Saccharomyces cerevisiae. (A. Caudy, Ed.). PLoS Genet. 12: e1006372.

Scalcinati, G., J. M. Otero, J. R. H. Vleet, T. W. Jeffries, L. Olsson *et al.*, 2012 Evolutionary engineering of Saccharomyces cerevisiae for efficient aerobic xylose consumption. FEMS Yeast Res. 12: 582–597.

SCHAAFF-GERSTENSCHLAGER, I., G. MANNHAUPT, I. VETTER, F. K. ZIMMERMANN, and H. FELDMANN, 1993 TKL2, a second transketolase gene of Saccharomyces cerevisiae. Cloning, sequence and deletion analysis of the gene. Eur. J. Biochem. 217: 487–492.

Schüller, H.-J., 2003 Transcriptional control of nonfermentative metabolism in the yeast Saccharomyces cerevisiae. Curr. Genet. 43: 139–60.

Shen, Y., J. Hou, and X. Bao, 2013 Enhanced xylose fermentation capacity related to an altered glucose sensing and repression network in a recombinant Saccharomyces cerevisiae. Bioengineered 4: 435–7.

Tamari, Z., D. Rosin, Y. Voichek, and N. Barkai, 2014 Coordination of gene expression and growth-rate in natural populations of budding yeast. (J. Mata, Ed.). PLoS One 9: e88801.

Velagapudi, V. R., C. Wittmann, K. Schneider, and E. Heinzle, 2007 Metabolic flux screening of Saccharomyces cerevisiae single knockout strains on glucose and galactose supports elucidation of gene function. J. Biotechnol. 132: 395–404.

Vemuri, G. N., M. A. Eiteman, J. E. McEwen, L. Olsson, and J. Nielsen, 2007 Increasing NADH oxidation reduces overflow metabolism in Saccharomyces cerevisiae. Proc. Natl. Acad. Sci. 104: 2402–2407.

Voichek, Y., R. Bar-Ziv, and N. Barkai, 2016 Expression homeostasis during DNA replication. Science (80-. ). 351:.

Wang, Y., M. Pierce, L. Schneper, C. G. Güldal, X. Zhang *et al.*, 2004 Ras and Gpa2 Mediate One Branch of a Redundant Glucose Signaling Pathway in Yeast (Paul Spellman, Ed.). PLoS Biol. 2: e128.

Zaman, S., S. I. Lippman, L. Schneper, N. Slonim, and J. R. Broach, 2009 Glucose regulates transcription in yeast through a network of signaling pathways. Mol. Syst. Biol. 5: 245.

Zaman, S., S. I. Lippman, X. Zhao, and J. R. Broach, 2008 How *Saccharomyces* Responds to Nutrients. Annu. Rev. Genet. 42: 27–81.

Zhang, M.-M., X.-Q. Zhao, C. Cheng, and F.-W. Bai, 2015 Improved growth and ethanol fermentation of *Saccharomyces cerevisiae* in the presence of acetic acid by overexpression

of *SET5* and *PPR1*. Biotechnol. J. 10: 1903–1911.

van Zyl, W. H., L. R. Lynd, R. den Haan, and J. E. McBride, 2007 Consolidated Bioprocessing for Bioethanol Production Using Saccharomyces cerevisiae, pp. 205–235 in *Advances in biochemical engineering/biotechnology*,.

# Figure Captions

**Figure 1 – Ethanol production on xylulose differs from glucose and galactose in yield and variability**

A. A schematic overview of carbon metabolism pathways in yeast. Shown are the major metabolic pathways discussed, which include the genes included in our screen.
B. Wild type cells produce different amounts of ethanol from different carbon sources. Shown are the amounts of ethanol produced by wild type yeast grown on SC media with each of the three carbon sources used in the screen. Cells were grown until all of the sugar in the media was consumed (24 hours on glucose, 40 hours on galactose, 13 days on xylulose) and the amount of ethanol produced was measured by HPLC analysis.
C. Variability of ethanol production differs dependent on carbon source. The amount of ethanol produced by each of the deletion strains during growth on each of the carbon sources examined is shown vs. their final OD at stationary phase. The color code depicts the percentage of growth rate of the wild type strain, as determined by a sensitive competition assay.

**Figure 2 – Genes essential for growth on xylulose are mostly required for growth on non-fermentable carbon sources**

A. Genes essential for growth on xylulose are mostly essential for growth on galactose and glycerol as well. Left panel: pathways to which the genes essential for growth on xylulose and galactose or xylulose and glycerol belong. Indicated in parentheses is the number of genes essential for growth on the carbon sources denoted (Gal = galactose, Gly = glycerol). Right panel: a scheme of glycolysis and the pentose phosphate pathway, in which the four genes required for growth on xylulose specifically are highlighted (red).
B. Growth on xylulose up regulates genes of the TCA cycle and electron transport chain. Shown is log(expression) on xylulose vs. log(expression) on glucose of genes of the TCA cycle and electron transport chain. A t-test was used to calculate the significance of the shift in the mean of the distribution relative to zero, giving a p-value of $1.82*10^{-6}$.
C. Growth on xylulose up regulates gluconeogenic genes. Shown is log(expression) on xylulose vs. log(expression) on glucose of genes of glycolysis, gluconeogenesis and the pentose phosphate pathway.
D. The expression pattern of genes of the TCA cycle, electron transport chain and pentose phosphate pathway during growth on xylulose correlates with that of cells growing on ethanol. Expression data for all carbon sources other than xylulose was taken from Gasch et al., 2000.
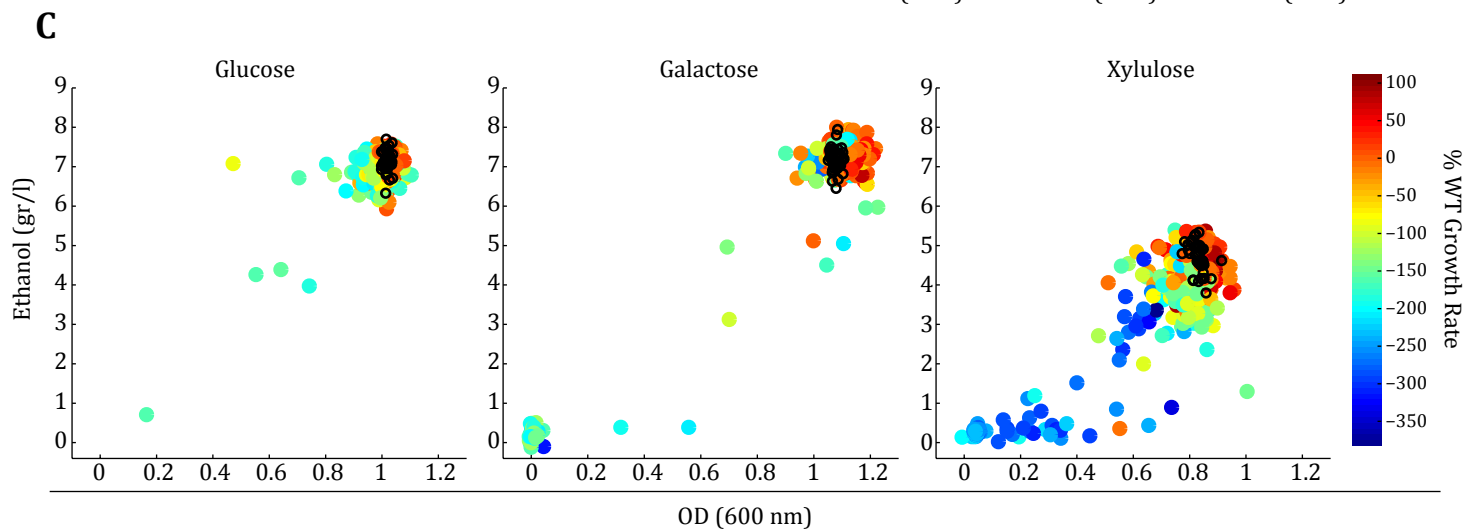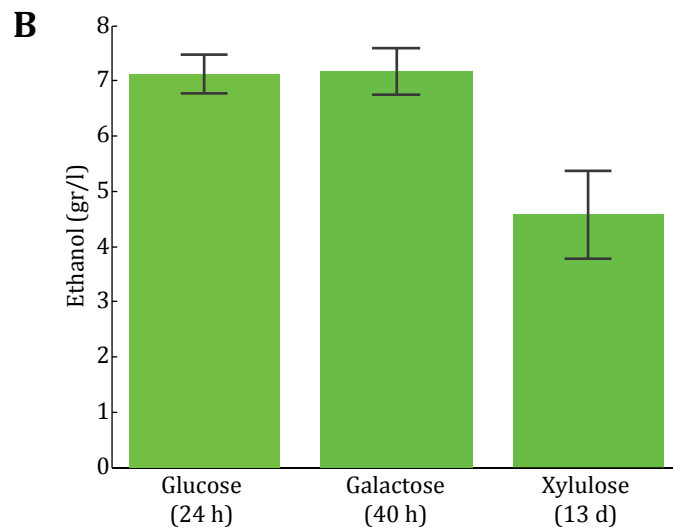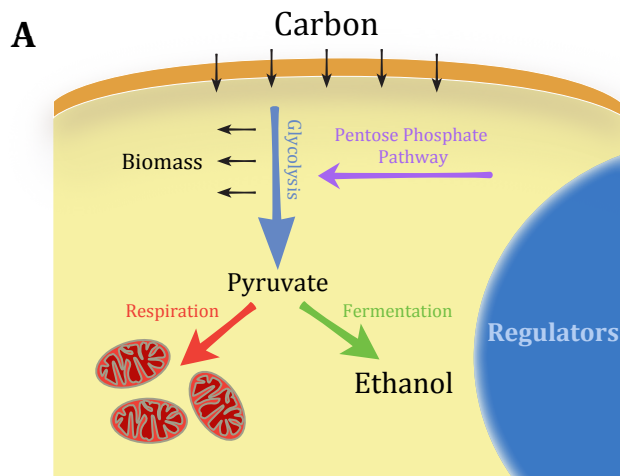
**Figure 3 – Mutant strains whose ethanol production phenotype differs from the wild type show wild type-like expression patterns**
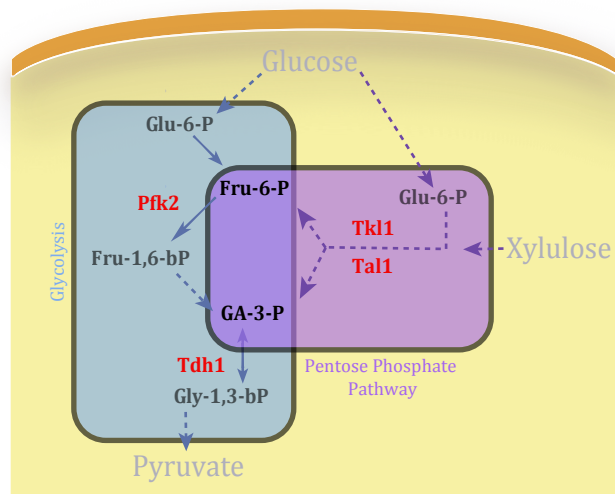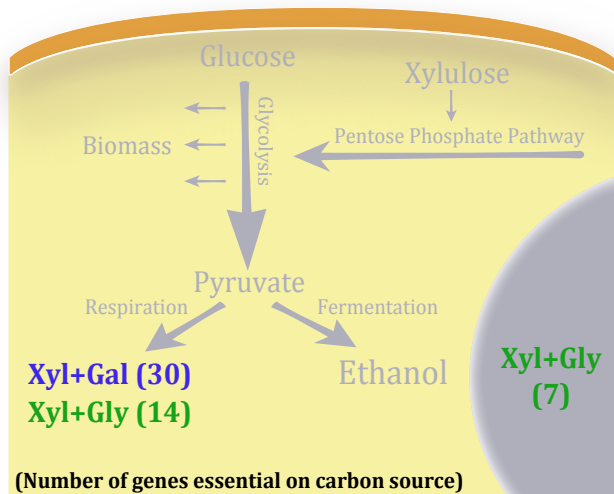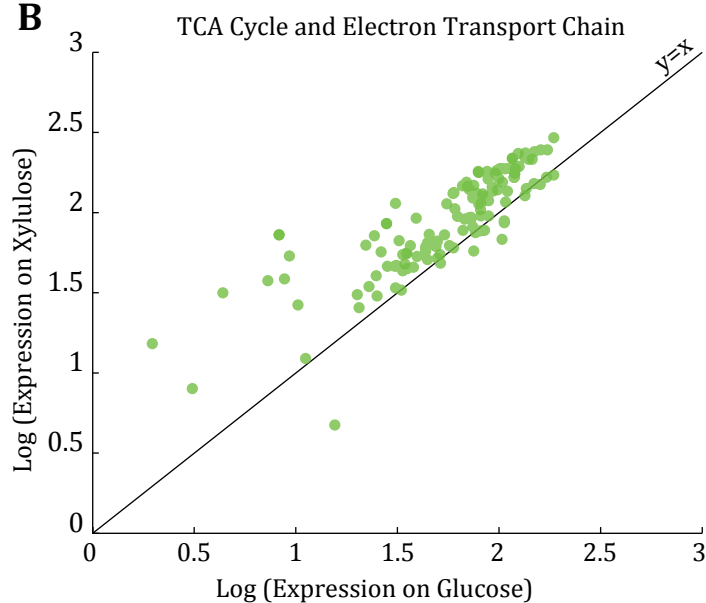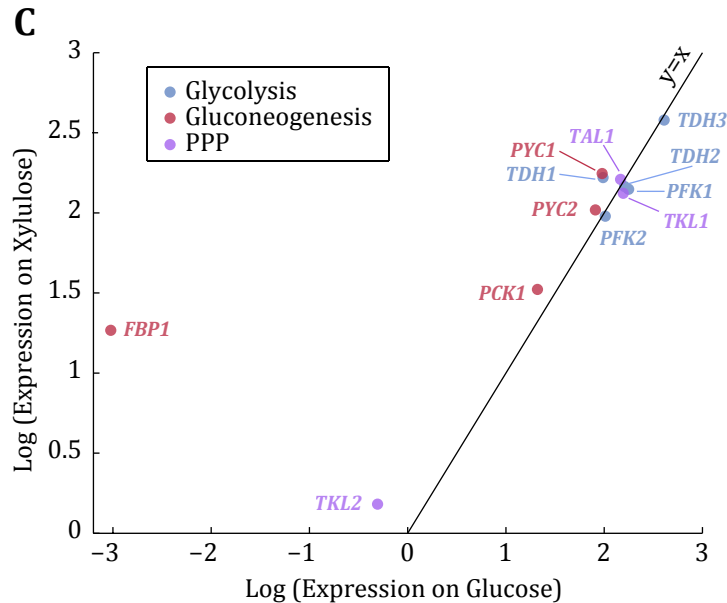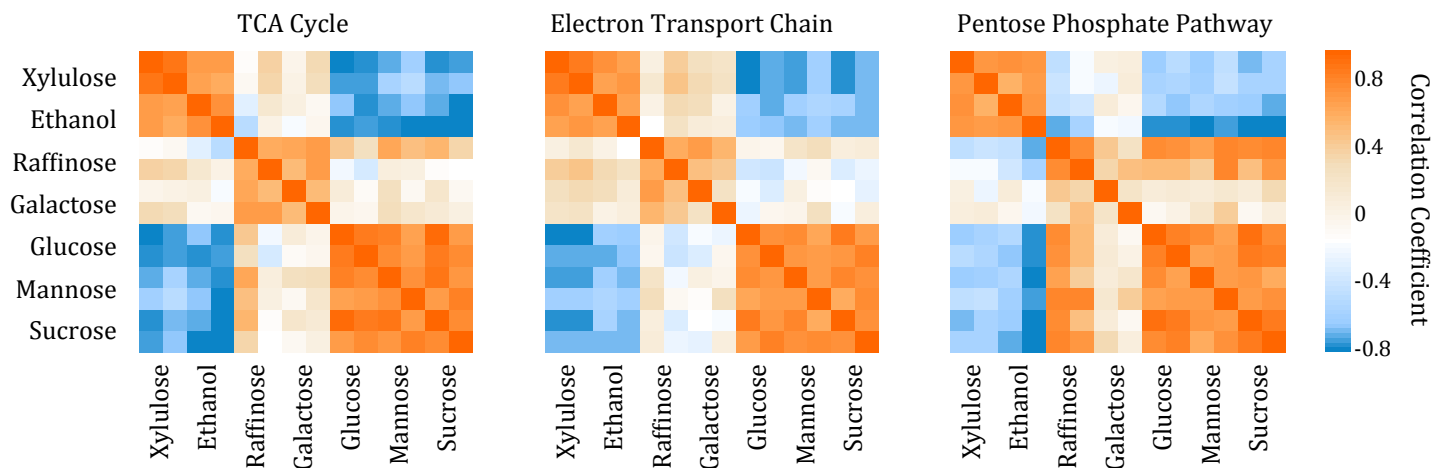
A. A schematic overview of the twenty validated candidate genes in the context of the pathways they take part of.
B. An example of a strain that produces less ethanol than the wild type at a lower final OD, ⊿*xks1*. Shown is the specific ethanol productivity of the mutant (red) vs. the wild type (black) reached after 7, 10 and 13 days of growth on xylulose.
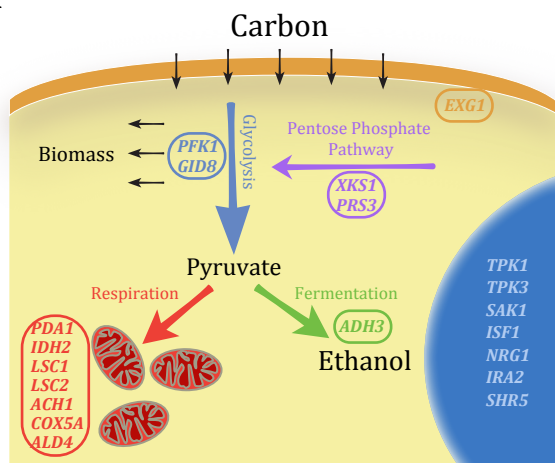
C. An example of a strain that produces less ethanol than the wild type at the same final OD reached by the wild type, *Δald4*. Shown is the specific ethanol productivity of the mutant (red) vs. the wild type (black) reached after 7, 10 and 13 days of growth on xylulose.

D. An example of a strain that produces ethanol amounts similar to that of the wild type at a lower final OD, *Δira2*. Shown is the specific ethanol productivity of the mutant (red) vs. the wild type (black) reached after 7, 10 and 13 days of growth on xylulose.
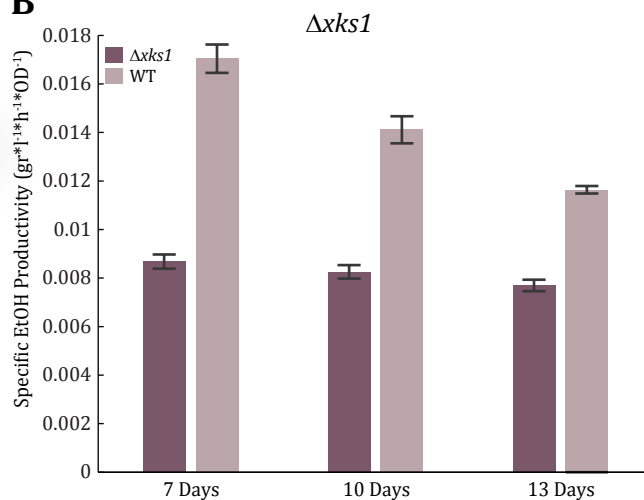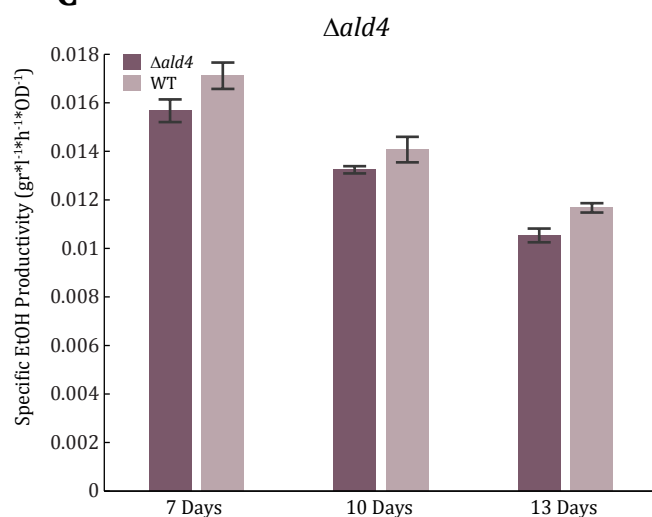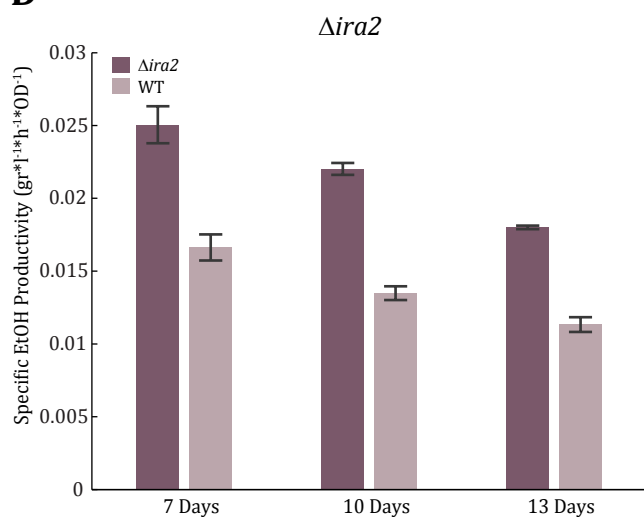
E. The gene expression of the different mutants resembles that of the wild type strain. Shown is the difference (log ratio) between expression on xylulose and expression on glucose of genes of the TCA cycle, pentose phosphate pathway (PPP) and electron transport chain (left) and amino acid biosynthesis (AA), ribosomal proteins (RP), ribosomal biogenesis (Ribi), ESR reduced, ESR induced and stress genes. Data is shown for wild type strains as well as all mutants examined. Gene groups as described in Tamari et al., 2014.

**Figure 4 – Mutant expression patterns do not correlate with ethanol production, growth rate or phenotype**

A. Mutant expression patterns do not correlate with ethanol production. Shown is a bar plot of the correlation between mean expression levels of genes belonging to the TCA cycle, electron transport chain and pentose phosphate pathway vs. the amount of ethanol produced by each deletion strain. Expression is defined as the difference (log ratio) between each deletion strain and the wild type.

B. Mutant expression patterns do not correlate with growth rate. Shown is a bar plot of the correlation between mean expression levels of genes belonging to the ESR induced, ESR reduced, amino acid biosynthesis (AA), ribosomal proteins (RP), ribosomal biosynthesis (Ribi), and stress genes vs. the strains' growth rate compared to the wild type. Expression is defined as the difference (log ratio) between each deletion strain and the wild type.

C. Specific ethanol productivity of *Δira2*, *Δidh2* and *Δpfk1* when grown on xylulose over time. Shown is the specific ethanol productivity after 7, 10, and 13 days of growth for each of the mutants as well as the wild type.

D. Expression patterns of *Δira2*, *Δidh2* and *Δpfk1* during logarithmic growth on xylulose. Difference (log ratio) between expression on xylulose of each deletion strain and the wild type, of genes belonging to the amino acid biosynthesis (AA), ribosomal proteins (RP), ribosomal biosynthesis (Ribi), ESR reduced, ESR induced and stress gene modules.

E. Specific ethanol productivity positively correlates with growth rate. Shown is specific ethanol productivity measured after 7 days of growth vs. percent of wild type growth rate for all mutants screened. Candidate mutants whose phenotype was validated are depicted in red.

**A**

Carbon

Biomass

Glycolysis

Pentose Phosphate Pathway

Pyruvate

Respiration          Fermentation

Ethanol

Regulators

**B**

**C**

Glucose          Galactose          Xylulose

Ethanol (gr/l)

OD (600 nm)

% WT Growth Rate

**A**

Glucose → Glycolysis → Biomass
Xylulose → Pentose Phosphate Pathway
Pyruvate → Respiration / Fermentation → Ethanol

Xyl+Gal (30)
Xyl+Gly (14)
Xyl+Gly (7)

(Number of genes essential on carbon source)

Glucose
Glu-6-P
Pfk2
Fru-6-P
Fru-1,6-bP
Glu-6-P
Tkl1
Tal1
Xylulose
GA-3-P
Glycolysis
Pentose Phosphate Pathway
Tdh1
Gly-1,3-bP
Pyruvate

**B** — TCA Cycle and Electron Transport Chain
X-axis: Log (Expression on Glucose)
Y-axis: Log (Expression on Xylulose)
y=x

**C**
X-axis: Log (Expression on Glucose)
Y-axis: Log (Expression on Xylulose)
y=x

Legend:
- Glycolysis
- Gluconeogenesis
- PPP

Labels: TDH3, TAL1, TDH2, PYC1, TDH1, PFK1, TKL1, PYC2, PFK2, PCK1, FBP1, TKL2

**D**
TCA Cycle | Electron Transport Chain | Pentose Phosphate Pathway

Rows/Columns: Xylulose, Ethanol, Raffinose, Galactose, Glucose, Mannose, Sucrose

Correlation Coefficient (0.8 to -0.8)

**A** Carbon

Biomass ← 
Glycolysis
PFK1 GID8
Pentose Phosphate Pathway
XKS1 PRS3
EXG1

Pyruvate
Respiration / Fermentation
PDA1 IDH2 LSC1 LSC2 ACH1 COX5A ALD4
ADH3
Ethanol

TPK1 TPK3 SAK1 ISF1 NRG1 IRA2 SHR5

**B** Δxks1

**C** Δald4

**D** Δira2

**E**

Log(exp(Xyl)/exp(Glu))

**A**

**B**

**C**
- Δidh2
- Δira2
- Δpfk1
- WT

**D**

Log(exp(mut)/exp(WT))

Stress + ESR Induced

RP + Ribi + ESR Reduced

AA

Δidh2    Δira2    Δpfk2

**E**

Δach1

Δidh2    Δira2

Δsak1

Δshr5    Δgid8    Δadh3    Δlsc2

Δtpk3    Δlsc1

Δnrg1

Δcox5a    Δald4

Δpfk1    Δpda1    Δtpk1

Δisf1    Δprs3    Δexg1    Δxks1